Brain-Machine Interface Driven Post-stroke Upper-limb Functional Recovery Correlates with Beta-band Mediated Cortical Networks

Dheeraj Rathee* *Student Member, IEEE*, Anirban Chowdhury *Student Member, IEEE*, Yogesh Kumar Meena *Member, IEEE*, Ashish Dutta *Member, IEEE*, Suzanne McDonough, Girijesh Prasad *Senior Member, IEEE*

Abstract—Brain-machine interface (BMI) driven robot-assisted neurorehabilitation intervention has demonstrated improvement in upper-limb (UL) motor function, specifically, with post-stroke hemiparetic patients. However, neurophysiological patterns related to such interventions are not well understood. This study examined the longitudinal changes in band-limited resting-state (RS) functional connectivity (FC) networks in association with post-stroke UL functional recovery achieved by a multimodal intervention involving motor attempt (MA) based BMI and robotic hand-exoskeleton. Four adults were rehabilitated with the intervention for a period lasting upto 6 weeks. RS magnetoencephalography (MEG) signals, Action Research Arm Test (ARAT), and grip strength (GS) measures were recorded at five equispaced sessions over the intervention period. An average post-interventional increase of 100.0% ($p = 0.00028$) and 88.0% were attained for ARAT and GS, respectively. A cluster-based statistical test involving correlation estimates between beta-band ($15-26$ Hz) RS-MEG FCs and UL functional recovery provided positively correlated sub-networks in both contralesional and ipsilesional motor cortices. The fronto-parietal FC exhibited hemispheric lateralisation wherein majority of the positively and negatively correlated connections were found in contralesional and ipsilesional hemispheres, respectively. Our findings are consistent with the theory of bilateral motor cortical association with UL recovery and predict novel FC patterns that can be important for higher level cognitive functions.

Index Terms—Hand neurorehabilitation, Functional brain networks, Magnetoencephalography, Motor attempt, Brain-computer interface, Hand-exoskeleton.

I. INTRODUCTION

Recovery of movement related functions after stroke and its assessment are highly crucial for restoring activities of daily living (ADLs) of the patients. Majority of the stroke survivors have upper-limb (UL) associated symptoms after undergoing an acute stroke [1]. Many patients show some degree of spontaneous (autonomous) recovery during initial months following a stroke, however, this is generally inadequate particularly in terms of motor functions. The condition

of the patients with null or incomplete recovery can be improvised with several restorative therapy methods. These methods mainly include: (i) dynamic splinting which helps the stroke survivors to straighten their wrists and fingers (e.g. physical therapy, constraint-induced movement therapy, gait therapy) [2], [3], (ii) electrical muscle stimulation (EMS) which helps in moving weak limb by using electric impulses delivered directly to skin using electrodes [4], [5], (iii) device-driven therapy which guides the users to execute repeated movements (e.g. robotics, brain-computer interface (BCI)) [6]–[9], (iv) transcranial magnetic stimulation (TMS) which uses electromagnetic induction to induce weak currents and helps in causing activity in specific parts of brain [10], [11], and (v) mirror therapy: to make it appears as if stroke survivors are moving their affected arm, however, they actually look at the movement of their unaffected hand [12], [13]. These days mental practice (MP) and physical practice (PP) are two frequently used evidence-based clinical interventions to enhance UL motor function purportedly to improve motor movement, coordination, and balance following stroke [14], [15].

Motor-imagery (MI) based BCI systems offer the use of neuronal signals i.e. Electroencephalography (EEG)/Magnetoencephalography (MEG) for UL rehabilitation goals, by providing the end users with brain state-related sensory feedback through various means such as functional electrical stimulation, virtual reality environments, or robotic systems. Taking this into consideration, BCI systems that are applied for motor neuromodulation purposes are used to induce activity-dependent plasticity by making the user pay close attention to a task requiring the activation or deactivation of specific brain areas [16]–[18]. Moreover, recent advancements in the EEG/MEG-driven stroke rehabilitation showed the significant efficacy of visual and proprioceptive feedback and robotic UL exoskeletons along with MI [19]–[22]. Furthermore, several other studies reported on using BCI-driven exoskeletons in patients with post-stroke UL paresis [23]–[26]. These studies involved various types of end-effector based haptic and kinesthetic feedback systems to improve the clinical parameters of post-stroke motor recovery e.g. a haptic knob [21], MIT Manus [27], and a custom-made orthotic device [26], [28], [29]. While an increasing number of studies have shown significant alterations in neural activations and functional connectivity networks related to the mental imagery and attempted movements

TABLE I
PARTICIPANT DETAILS: THE ID, AGE, SEX, AFFECTED HEMISHPERE, MINI-MENTAL STATE EXAMINATION (MMSE) SCORE, TIME SINCE STROKE, BASELINE ARAT SCORE, BASELINE GS SCORE AND AFFECTED BRAIN LOCATION ARE SHOWN FOR EACH PARTICIPANT. *P05 HAD TO LEAVE THE INTERVENTION AFTER INITIAL 2 WEEKS OF THE INTERVENTION.

Participant ID	Age (years)	Sex	Affected Upper limb	MMSE score	Time since stroke (months)	Baseline ARAT	Baseline GS (Kgs)	Most affected brain location
P01	56	M	Left	30	28	6	11.7	Right middle cerebral artery
P02	69	F	Right	28	24	29	13.7	Left frontal lobe peri-ventricular and basal gangalia region
P03	60	F	Right	28.5	22	35	3	Left side of pons
P04	65	F	Left	27	18	24	12	Thalamus
P05	58	M	Right	28	17	26	13.3	Brainstem
Mean (SD)	61.6 (5.3)			21.8 (4.5)	28.3 (1.1)	24 (10.9)	10.7 (4.4)	

of an impaired upper extremity (i.e. Motor attempt (MA)) with the use of neural signal driven-robotic devices [19], [28], [30], [31], it still remains unclear whether and to what extent the underlying neurophysiological mechanisms are affected during a UL stroke rehabilitative intervention using an MA-related EEG-driven hand-exoskeleton.

Nevertheless, there are three major limitations of the currently available functional connectivity-based studies implemented for validation of the clinical efficacy of EEG-based rehabilitative interventions. Firstly, the majority of these studies are focused on the reorganisation of brain networks during the MI and execution task and thus, include the issue of controlling for effort and performance when stroke patients with varying motor deficits are under consideration [32], [33]. Secondly, the comparisons are drawn on the brain networks between the pre- and post-intervention states, thus, failed to observe the continuous change patterns in the brain networks during the course of the rehabilitative intervention [19], [34]. Lastly and most importantly, none of the previous studies attempted to examine brain network-based neurophysiological changes for a multi-modal longitudinal rehabilitation intervention involving the simultaneous implementation of MA, BCI, visual and proprioceptive feedbacks, and robotic hand-exoskeleton. Thus, there is a pressing need to examine the brain functional networks that are correlated with the motor recovery during a longitudinal multimodal post-stroke UL rehabilitative intervention.

In this paper, we estimated the brain connectivity networks using resting-state (RS) MEG signals acquired at five different sessions in conjunction with a multi-modal rehabilitative therapy provided with the simultaneous intervention of MA-based BCI and robotic hand-exoskeleton over a period of upto 6 weeks. This study included five sessions of behavioural assessment involving Action Research Arm Test (ARAT) and grip-strength (GS) tests. Further, to assess the neural mechanisms related to the stroke recovery obtained from BCI-driven robotic hand-exoskeleton, the associations between the estimated brain networks of the RS MEG data and the behavioural outcomes are evaluated.

The remainder of this paper is organized as follows: Section II provides the detailed description about the participants, rehabilitative intervention, assessment of UL functional recov-

ery, and acquisition and connectivity analysis of RS MEG data. Section III presents the outcomes of the UL functional recovery assessment, BCI performance in terms of classification accuracies, and the RS MEG connectivity analysis. Section IV discusses the outcomes, impact, and limitation of this study along with possible future enhancements.

II. MATERIALS AND METHODS

A. Participants

Five stroke (ischemic) survivors (3 females, 2 males, age 61.6 ± 5.32 years (range $56-69$ years)) who had persistent coordination deficit of the UL were enrolled for an uncontrolled clinical trial. The clinical trial is retrospectively registered at the ISRCTN registry with the registration number *ISRCTN13139098*[1]. The mean time after stroke was 21.8 ± 4.49 months (range $17-28$ months). Table I provides the demographic information of all the participants. Four participants were first-time stroke victims. All participants provided written informed consent for their participation and this study was approved by the University Research Ethics Committee of the Ulster University, Northern Ireland, UK. All research procedures were carried out in accordance with approved institutional guidelines and regulations. Inclusion criteria were as follows: ischemic stroke resulting in UL disability, time since stroke onset greater than 6 months, age between $18-80$ years (both inclusive), and no history of neurological condition. Exclusion criteria were as follows: severe deficits in cognition (Mini-Mental State Examination (MMSE) score <21), claustrophobic, pregnant or breastfeeding, and metal or active body implants. As one of the participants (i.e. P05) had to leave the intervention after initial 2 weeks of the intervention, the data of the participant is excluded from the analysis.

B. Intervention

In this study, we have conducted a clinical trial comprising of a rehabilitative intervention to four hemiparetic stroke patients who underwent the same intervention for a period of upto 6 weeks. The intervention consisted of two stages.

[1]http://www.isrctn.com/ISRCTN13139098
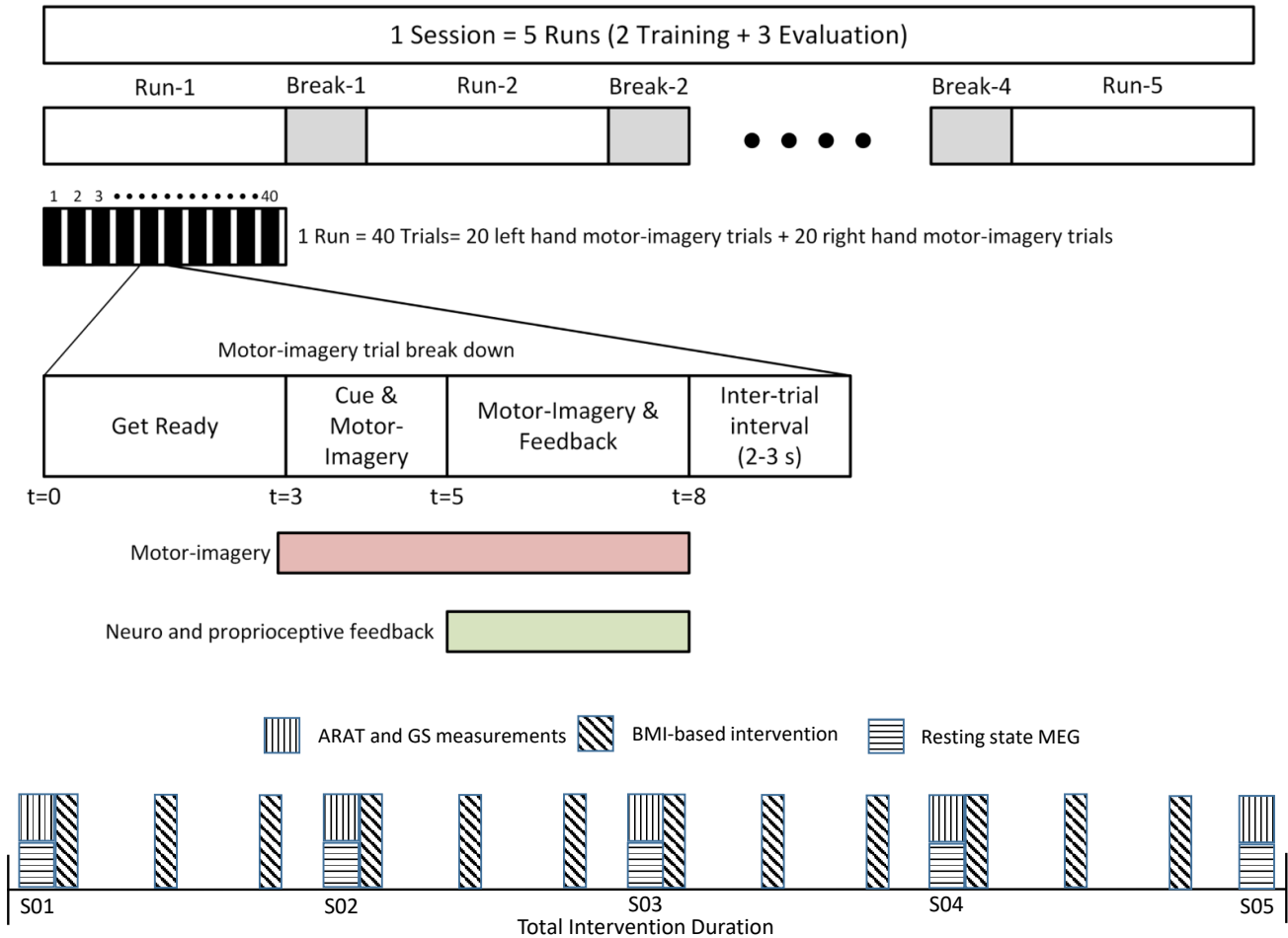
Fig. 1. A detailed description of proposed EEG and MEG data acquisition paradigm. The upper section provides the description of the BMI paradigm. The lower section presents the timings of BMI-based intervention, rehabilitation outcome assessment (i.e. ARAT and GS), and RS MEG data acquisition over the total duration of the rehabilitative intervention (upto 6 weeks). ARAT, GS, and RS MEG were recorded at five different sessions (S01−S05).

The first stage was the PP stage of 30 min immediately followed by a MP stage of almost 46 min including the BCI calibration time of around 16 min. This PP and MP based neurorehabilitation protocol was inspired by our earlier works on BCI based UL rehabilitation producing effective motor recovery [35].

The PP stage was of 30 min duration during which a home-grown hand-exoskeleton device provided repetitive finger grasping and extension exercise to the affected hand in assist-as-needed mode. The assist-as-needed strategy was implemented by a force threshold based switching between active non-assist and passive assistance mode. The applied fingertip force by the participants was converted into exoskeleton motion using an impedance model when the force is above a certain threshold level (active non-assist mode). The controller goes into a passive assistance mode providing full assistance to complete the on-going finger grasping/extension action when the applied force is below the threshold. The difficulty level of the PP was adjusted by updating the impedance parameters of the controller, according to the average force generation ability of the participant in a session.

In the MP stage the participants were given a hybrid-BCI

based multimodal neurofeedback contingent to the simultaneous activations in the EEG and electromyography (EMG) signal measured by a spectral bandpower correlation between the two [36]. Fig. 1 depicts the timing and structural details of MP stage of the intervention. In one particular session of the MP, there were five runs of approximately 7 min 3 s each consisting of 40 trials. Each trial starts with a 3 s rest period, followed by the presentation of a cue to perform either a left or right-hand grasp attempt. Although the cue remains for 2 s, the participants were asked to perform the task until 5 s after the presentation of the cue. Among the 5 runs, first 2 runs were for calibrating the BCI system and the subsequent 3 runs were for giving online neurofeedback based on the EEG-EMG pattern classifier trained during the calibration stage. For the online neurofeedback runs, visual and proprioceptive feedbacks were provided through the screen and hand-exoskeleton, respectively, during the last 3 s of the task period. The exoskeleton was worn in the impaired hand of the participant, whereas the other hand was placed on a softball on top of the table. During the task period of the trials, the participants were asked either to perform the grasp movement with the hand-exoskeleon with impared hand or with softball with unimpaired hand and the

subsequent visual feedback was provided in both cases. It is to be noted that the participants had not gone for any kind of physiotherapy (PT) or occupational therapy (OT) during the course of the intervention.

C. Rehabilitation Outcome Measures

Each participant underwent the ARAT [37] and GS assessment at five different times during the complete duration of the intervention. The ARAT is a standardized ordinal scale for the assessment of 4 basic UL movements i.e. primary grasp (score range: $0-18$), grip (score range: $0-12$), pinch (score range: $0-18$), and gross movements of flexion and extension at the elbow and shoulder (score range: $0-9$). GS (in Kg) was assessed using a hydraulic hand dynamometer which gives accurate and repeatable GS readings. The hydraulic hand dynamometer provides five different positions to accommodate variable hand sizes and features a range of 0 to 200lb (90kg). While GS is used to directly describe strength of the UL, it may also indicate the level of overall upper extremity strength. Participants were seated with the upper extremity in $0°$ of shoulder flexion and $90°$ of elbow flexion. At each session, 3 measurements were taken, and the average value was used in the analyses.

D. MEG Acquisition

All the participants were screened for any metallic foreign substance e.g. jewellery, coins, keys or any other ferromagnetic material before entering the magnetically shielded room. The standard fiducial landmarks (left and right pre-auricular points and Nasion), five head position indicator (HPI) coils (placed over scalp), and the additional reference points over the scalp were digitised (Fastrak Polhemus system) to store information about the participant's head position, orientation, and shape. In addition, ocular and cardiac activities were recorded with two sets of bipolar electro-oculogram (EOG) electrodes (horizontal-EOG and vertical-EOG) and one set of electrocardiogram (EKG) electrodes, respectively. Before starting the data acquisition, the complete procedure and the experimental paradigm were described to the participants.

Ten minutes of resting-state MEG data (i.e. five minutes each for eyes-open and eyes-closed) were recorded with a 306-channel (102 magnetometers and 204 planar gradiometers) Elekta Neuromag^{TM} system (Elekta Oy, Helsinki, Finland) located at the Northern Ireland Functional Brain Mapping (NIFBM) Facility of the Intelligent Systems Research Centre, Ulster University. During the eyes-open experiment participants were instructed to remain relaxed but alert with their eyes open and fixated on a red cross presented at the centre of the screen. The fixation point was displayed on a Panasonic projector with a screen resolution of 1024×768 and refresh rate of 60 Hz. All recordings were made with participants seating in upright position in the scanner.

The MEG signals were filtered at a bandwidth of $0.1-330$ Hz (online) and sampled at the rate of 1 kHz during the acquisition itself. Continuous head positioning was switched on after 20 s of raw data recording and kept running for rest of the acquisition period.

E. MEG Analysis

Pre-processing and Independent Component Analysis: During the rehabilitative intervention, a total of five sessions of MEG datasets were recorded for each participant. As several participants reported episodes of sleep during eyes-closed paradigm, only RS eyes-open MEG data have been included for further analysis. The recorded datasets were visually examined for strong muscular movements, and then processed for head movement correction wherein HPI signal-based compensation was carried out using an inbuilt software i.e. Maxfilter in the ELEKTA MEG system (Elekta Neuromag Oy, version 2.2.15). The environmental interferences and constant or periodic artefacts were corrected by applying the temporal extension of signal-space separation (t-SSS) method with default parameters and after exclusion of bad channels [38]. Further to this point, data processing was performed using the FieldTrip toolbox [39] and Matlab 9.2 (64 bit version, R2017a, Mathworks, Natick, USA).

The data were bandpass filtered over $1-145$ Hz and notch filtered at harmonics of 50 Hz (i.e. 50 and 100 Hz). Artefacts related to squid jump, clip, and muscular movements were identified and removed. The cleaned data were then decomposed into independent components (ICs) by means of the FastICA algorithm [40] and ICs related to EOG and EKG were identified using an in-house algorithm based on correlation and coherence methods. Before running the IC decomposition, the data were resampled to 500 Hz to reduce the computational load. The remaining ICs were further categorized into brain and non-brain ICs using their multiple characteristics (e.g. fit with 1/f spectrum, flat spectrum quantification, and time kurtosis) in time and frequency domains [41], [42]. The whole process was repeated 20 times and the iteration with highest number of brain ICs was selected for further analysis.

Source Localisation: The IC sensor maps were projected onto the individual participants' brain via a localization procedure carried out by means of a linear inverse method. The T1-weighted structural magnetic resonance images were obtained from each participant's health records after obtaining their consent. Further, the structural MRI of the participants' head was co-registered to the MEG coordinates using the three fiducial points and the scalp points acquired before the MEG data acquisition. A single shell volume conduction model was created based on the segmentation of the head tissues. The structural data was further processed using FreeSurfer [43], [44] and MNE suite [45] involving triagulation of the cortical surfaces with dense meshes with $\sim 4,000$ vertices in each hemisphere. This allows for the definition of the source space, that is, a regular 2D grid within the single shell head model, sampled into 8126 voxels corresponding to a spacing of approximately 8mm between adjacent source locations. A geometrical registration of the MEG sensor array to a coordinate system referred to the participants' head was performed by using functional landmarks (i.e. nasion and preauricular points). The m_c brain IC sensor maps were scaled to norm one. An amplitude restoring factor α_i, to be subsequently used in the forward model of data formation, is defined such as $a_{ci} = \alpha_i \widetilde{a}_{ci}$, where $\widetilde{a}_{ci}$ indicates the ith IC sensor-level
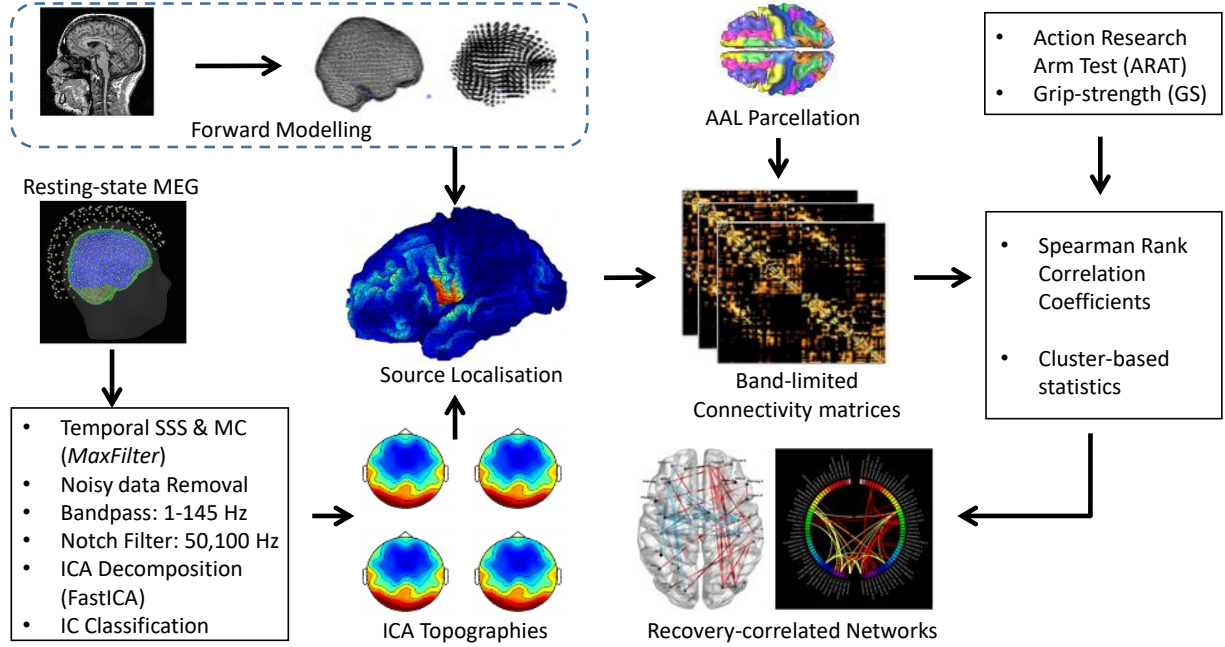
Fig. 2. Schematic illustration of the signal analysis pipeline. From top left corner: Resting state MEG data were preprocessed and then, decomposed to independent components (ICs) using FastICA. Further the IC classification was performed to obtain brain-related ICs. The topographies of brain ICs and forward model created from the structural MRI were utilised for source localisation of the MEG data. Further, band-limited voxel-based functional connectivity networks (FBNs) were generated and converted to ROI-based networks using AAL atlas. Next, cluster-based statistics was implemented to obtain the recovery-correlated functional sub-networks.

map after scaling. Next, the scaled IC sensors maps were projected onto the source space via a weighted minimum-norm least squares (WMNLS) inverse method [46], [47]. Thus, the brain IC source maps q_i are obtained from the sensor maps as follows:

$$q_i = W^{-2}L^T(LW^{-2}L^T + \lambda I)\widetilde{a}_{ci} \qquad (1)$$

where i runs over the subset of the m_c brain ICs, W is a diagonal weighting matrix of size $[3k \times 3k]$, the elements of which are defined by $W_{kk} = ||L||$, L is the lead-field matrix of size $[n \times 3k]$, I is the identity matrix of size $[n \times n]$, and λ is a regularization parameter set on the basis of the noise level [48]. In this analysis pipeline, the regularization parameter was optimized separately for each IC. This is an important difference with respect to WMNLS localization of artifact-corrected recordings. After the localization step, m_c source maps in participants' space were obtained. In addition, an affine transformation has been applied to the source maps for a coordinate transformation to an MNI stereotaxic space. This allowed spatial comparison across participants.

Once the component topographies had been projected on to the source space, the activity at each voxel and in each sample in time was obtained as a linear combination of the component time courses weighted by their related brain source map.

Functional Brain Network Estimation: For the estimation of functional connectivity networks from the source localised MEG data, we used an extension of the imaginary part of coherence, namely the Multivariate Interaction Measure

(MIM) [49], [50], that maximizes the imaginary part of coherence between a given reference voxel (seed, s) and any other voxel (target, j). More specifically, the estimated MEG signal at each brain voxel is a vector quantity that can be represented through its components in a given reference system. MIM is designed to maximize the imaginary part of coherence between vector quantities. The mathematical details on MIM derivation can be found in [49]. For the readers' convenience, we briefly review MIM definition in the following.

Given the vector Fourier transformed signals as a function of frequency f at the seed and target voxels: $X_s(f)$ and $X_j(f)$, respectively, and introducing the compact notation $X(f) = [X_s^T(f) X_j^T(f)]^T$, the cross-spectrum (C(f)) between the two vectors $X_s(f)$ and $X_j(f)$, can be written in the block form:

$$C(f) = \langle X(f)X(f)^* \rangle \qquad (2)$$

$$C(f) = \left[\begin{array}{cc} C_{ss}^R(f) + JC_{ss}^I(f) & C_{sj}^R(f) + JC_{sj}^I(f) \\ C_{js}^R(f) + JC_{js}^I(f) & C_{jj}^R(f) + JC_{jj}^I(f) \end{array} \right] \qquad (3)$$

and MIM between s and j is thus defined as:

$$MIM_{sj} = tr\left((C_{ss}^R)^{-1}C_{sj}^I(C_{jj}^R)^{-1}(C_{sj}^I)^T\right) \qquad (4)$$

In the above notation, tr indicates matrix trace, the T subscript indicates matrix transpose, superscripts R and I denote the real and the imaginary parts, the $(\cdot)^{-1}$ subscript indicates matrix inverse, the $*$ subscript indicates matrix conjugate transpose, and the capital J indicates the imaginary

unit. A more detailed recapitulation of the method is also given in Marzetti et al. (2013) [50].

In this work, cross-spectra were estimated with Fast Fourier analysis after signal linear de-trending and Hanning windowing and were averaged using time epochs of 1.0 s duration with 50% overlap leading to a frequency resolution of 1 Hz. The number of averaged epochs is approximately 550 for each dataset. The method, being based on the maximization of imaginary coherence, largely overcomes the well-known limitation to the study of functional connectivity by EEG/MEG posed by signal mixing artifacts, i.e., any active source in the brain contributes, in a weighted manner, to the signals measured at all sensors through volume spread (see Figure 2A in [51]). This effect constitutes an especially severe confound for estimates of brain interactions [52]–[55] and needs to be taken into account by mapping MEG functional connectivity through robust measures. Thus, voxel-wise whole brain networks in various frequency bands i.e., delta $(1-4$ Hz), theta $(4-8$Hz), alpha $(8-15$ Hz), beta-low $(15-26$ Hz), beta-high $(26-35$ Hz), gamma-low $(34-49$ Hz), gamma-mid $(51-76$ Hz) and gamma-high $(76-120$ Hz) were obtained using MIM with the reconstructed neuronal time-series. Furthermore, these voxel-based networks were parcellated to ROI-based networks using automated anatomical labelling (AAL) [56] atlas restricting the further analysis to 78 cortical regions and 12 sub-cortical brain regions. This process was implemented for all the MEG sessions and each participant to generate respective FBNs.

F. Cluster-based Statistical Testing

For estimating the overall upper limb functional recovery, we first estimated a composite recovery score by taking a weighted mean of the GS measure and the total ARAT score i.e. sum of the four components (primary grasp, grip, pinch, and gross movements). Firstly, the respective weights for both variables were calculated using following equations:

$$w_{ATAS} = 1 - \frac{mean_{ATAS}}{mean_{ATAS} + mean_{GS}} \qquad (5)$$

$$w_{GS} = 1 - \frac{mean_{GS}}{mean_{ATAS} + mean_{GS}} \qquad (6)$$

Secondly, the raw values of ATAS and GS were multiplied with their respective weights and averaged to generate the final composite score for each session. Next, given brain connectivity data, we implemented cluster-based statistics which is a two-step process, to estimate the sub-networks which are (un)correlated with the composite recovery score. In the first step, partial correlation coefficients between each edge of the FBN and the composite recovery score were computed using Spearman rank correlation coefficient since distribution of the brain connectivity data is unknown and often does not satisfy the normality condition. The second step of our method performs cluster-based multiple comparison correction for correlation coefficients computed in the previous step for all network edges. The neighbouring connections with strong correlation were first grouped together to form clusters and their maximum sizes were calculated. This procedure is repeated for randomly permuted assignments of composite

recovery score and finally significance levels of the identified sub-networks are estimated from the null distribution of the cluster sizes [57]. This method is independent of network construction methods: either structural or functional network can be used in association with any behavioural measures and its efficacy has been proved by several previous studies [58], [59].

It is worth noting that before implementation of the cluster-based statistical analysis, the ROIs for two participant who had right hemisphere lesions were flipped along the x-plane so that all lesions are on the left hemisphere, thus, for all participants, the left hemisphere is the ipsilesional hemisphere.
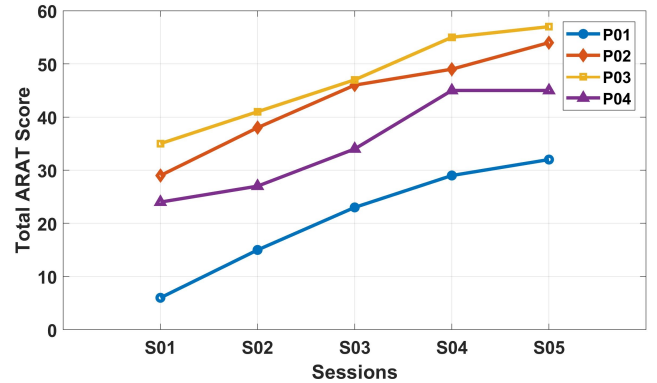
Fig. 3. The ARAT score recorded over the five sessions of the rehabilitative intervention for the four participants.
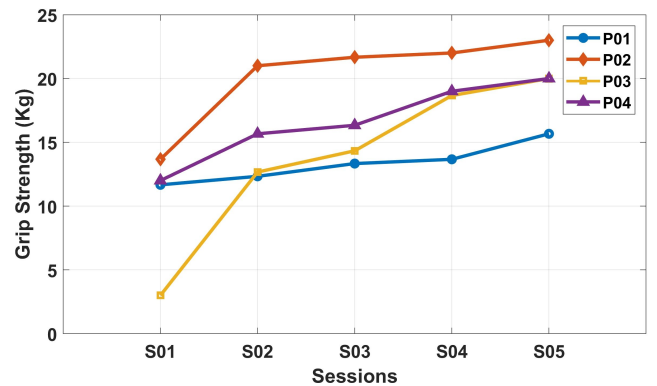
Fig. 4. The grip-strength (in Kg) recorded over the five sessions of the rehabilitative intervention for the four participants.

III. RESULTS

A. Assessment of Rehabilitation Outcome Measures

The total ARAT score and the GS (in kg) are measured five times during the intervention at regular intervals and their values over the five sessions and for all four participants are presented in Fig. 3 and Fig. 4, respectively. A steady increase in the ARAT score is observed for all the participants and the improvement is in range of 21 for P04 to 26 for P01. In a similar manner, GSs of all the participants are also improved over the course of intervention, however, in contrast to ARAT score, the incremental changes are highly variable. For P03, there is a high percentage increase in the GS (approximately
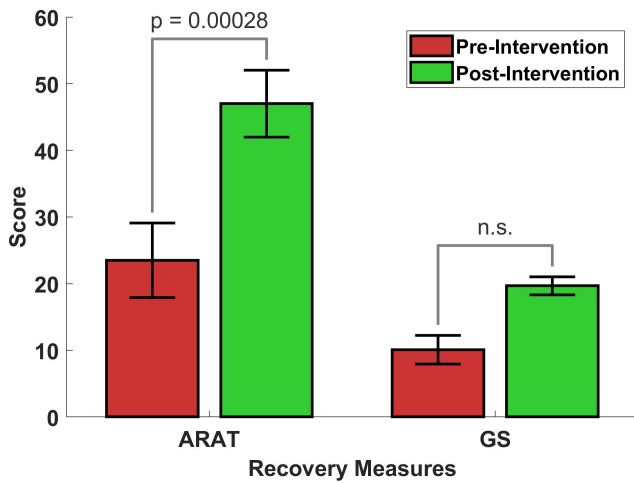
Fig. 5. The average ARAT and GS scores across four participants recorded before and after the rehabilitative intervention i.e. pre-intervention (red color) and post-intervention (green color). The error bar represents the standard error mean. Two-tailed, paired student t-test is implemented between pre- and post-intervention scores. n.s.- not significant.

600.0%) whereas the GS is comparatively less improved (approximately 30.0%) for P01. The GS improvement is in range of 1.7 Kg for P01 to 17 Kg for P03. Fig. 5 presents the average ARAT and GS scores across the four participants recorded before and after the rehabilitative intervention i.e. pre-intervention (red color) and post-intervention (green color). The error bar represents the standard error mean. Across all the participants, there is a mean change of 23.5 (100.0%) and 8.9 (88.0%) with respect to the mean score of 23.5 and 10.1 recorded at pre-intervention session for ARAT and GS, respectively. The student t-test (paired, two-tailed) is implemented to estimate the statistical significance for the change in pre- and post-intervention values of both parameters. The test provided statistically significant difference in the ARAT score only ($p = 0.00028$). Nevertheless, both measures showed improvements greater than the minimal clinically important difference (MCID). The MCID values for grip strength were reported as 5.0 and 6.2 kg and for ARAT as 12 and 17 points for the impaired dominant and nondominant upper-limb, respectively [60]. The total ARAT score and the GS (in kg) are measured five times during the intervention at regular intervals and their values over the five sessions and for all four participants are presented in Fig. 3 and Fig. 4, respectively. A steady increase in the ARAT score is observed for all the participants and the improvement is in range of 21 for P04 to 26 for P01. In a similar manner, GSs of all the participants are also improved over the course of intervention, however, in contrast to ARAT score, the incremental changes are highly variable. For P03, there is a high percentage increase in the GS (approximately 600.0%) whereas the GS is comparatively less improvised (approximately 30.0%) for P01. The GS improvement is in range of 1.7 Kg for P01 to 17 Kg for P03. Fig. 5 presents the average ARAT and GS scores across the four participants recorded before and after the rehabilitative intervention i.e. pre-intervention (red color) and post-intervention (green color). The error bar represents

the standard error mean. Across all the participants, there is a mean change of 23.5 (100.0%) and 8.9 (88.0%) with respect to the mean score of 23.5 and 10.1 recorded at pre-intervention session for ARAT and GS, respectively. The student t-test (paired, two-tailed) is implemented to estimate the statistical significance for the change in pre- and post-intervention values of both parameters. The test provided statistically significant difference in the ARAT score only ($p = 0.00028$). Nevertheless, both measures showed improvements greater than the minimal clinically important difference (MCID). The MCID values for grip strength were reported as 5.0 and 6.2 kg and for ARAT as 12 and 17 points for the impaired dominant and nondominant upper-limb, respectively [60].

TABLE II
THE MEAN NODE STRENGTHS OF ALL THE SIGNIFICANTLY CORRELATED AAL ATLAS BASED ROIS AND THEIR MNI COORDINATES.

AAL ROI	MNI Coordinates			Mean Node Strength
	X	Y	Z	($\times 10^{-3}$)
PreCG-L	-39	-6	51	4.26
PreCG-R	41	-8	52	3.51
SFGdor-L	-18	35	42	1.61
SFGdor-R	22	31	44	-4.46
ORBsup-L	-17	47	-13	-1.09
ORBsup-R	18	48	-14	-3.29
MFG-L	-33	33	35	2.73
MFG-R	38	33	34	-1.13
ORBmid-L	-31	50	-10	-1.48
ORBmid-R	33	53	-11	-0.52
IFGoperc-L	-48	13	19	1.35
IFGoperc-R	50	15	21	-1.02
IFGtriang-L	-46	30	14	1.65
IFGtriang-R	50	30	14	-2.75
ROL-R	53	-6	15	-2.09
SMA-L	-5	5	61	4.15
SMA-R	9	0	62	5.28
OLF-L	-8	15	-11	-1.44
SFGmed-L	-5	49	31	-0.5
SFGmed-R	9	51	30	-4.35
ORBsupmed-R	8	52	-7	-1.39
INS-R	39	6	2	-1.42
ACG-L	-4	35	14	0.96
ACG-R	8	37	16	-0.23
DCG-R	8	-9	40	-0.29
PCG-R	7	-42	22	-0.31
PHG-R	25	-15	-20	-1.5
LING-R	16	-67	-4	-1.27
SOG-L	-17	-84	28	0.28
SOG-R	24	-81	31	-1.56
MOG-L	-32	-81	16	-0.34
MOG-R	37	-80	19	-4.52
FFG-L	-31	-40	-20	-0.26
FFG-R	34	-39	-20	-2.81
PoCG-L	-42	-23	49	5.15
PoCG-R	41	-25	53	5.5
SPG-L	-23	-60	59	0.49
SPG-R	26	-59	62	-2.82
IPL-L	-43	-46	47	1.45
IPL-R	46	-46	50	-1.51
SMG-R	58	-32	34	-0.43
ANG-L	-44	-61	36	-0.52
ANG-R	46	-60	39	-0.19
STG-R	58	-22	7	-4.25
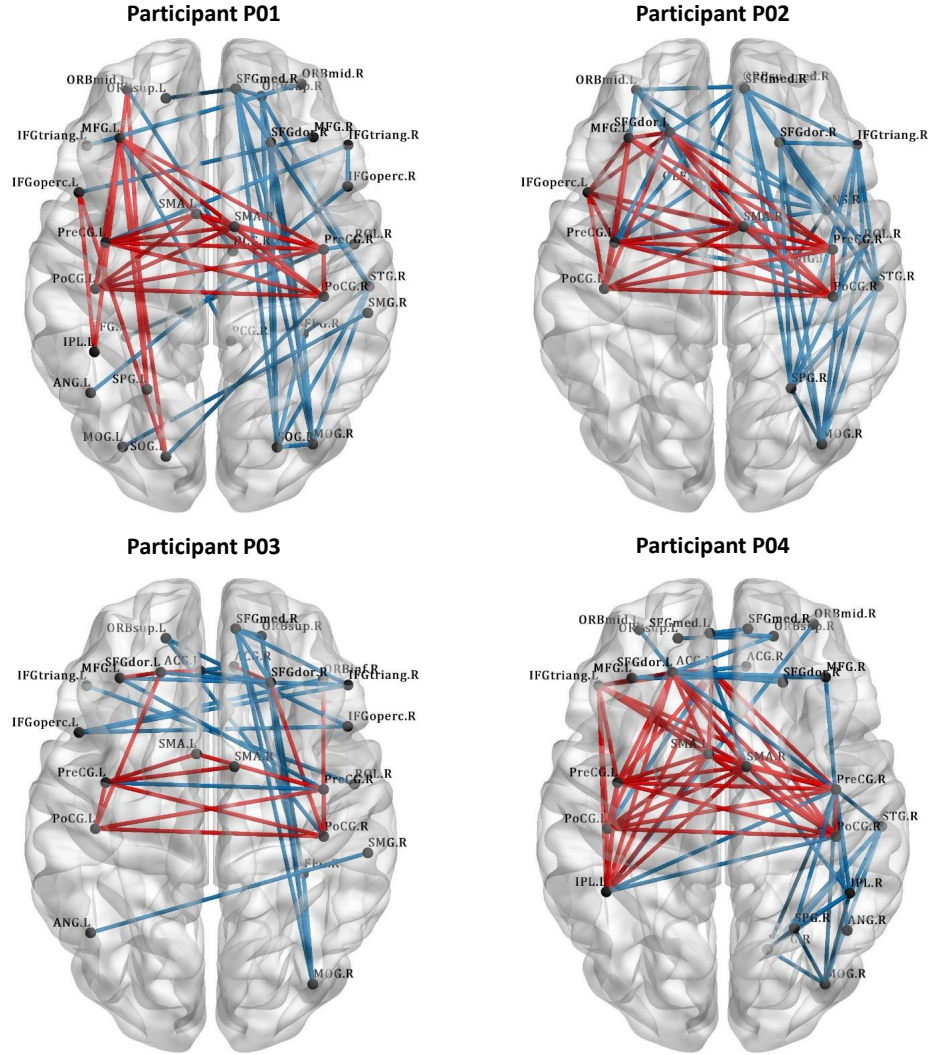
Fig. 6. Functional connectivity clusters correlated positively (Red) and negatively (Blue) with the UL functional recovery index for all four participants in beta-low (15−26 Hz) frequency band. Left = Ipsilesional hemisphere. The nomenclature of the AAL atlas brain regions and their list of abbreviations are provided in Table S1 of the supplementary document.

B. MEG Connectivity Analysis

The cluster-based statistical analysis provided significant functional connectivity sub-networks for alpha (8−15 Hz), beta-low (15−26 Hz), beta-high (26−35 Hz) frequency bands; however, these sub-networks are stable (i.e. presence of any positively/negatively correlated cluster over all the four participants) only for beta-low (15−26 Hz) band. Thus, the further results are presented for beta-low band, unless stated otherwise. Fig. 6 presents the positively and negatively correlated (with respect to UL functional recovery index) functional connectivity clusters for all four participants on a template brain. The black dots represent the ROIs based on the AAL atlas. For all the participants, the intra-hemispherical FC values in motor cortical regions involving precentral gyrus (i.e. primary motor area (M1)), postcentral gyrus (i.e. primary somatosensory cortex (S1)) and supplementary motor area (SMA) within both ipsilesional and contralesional hemispheres increase with UL functional recovery. However, this pattern exhibits inter-subject variability i.e. the positively correlated

FCNs are denser in case of P01, P02, and P04 as compared to P03 (see Fig. 6). The cluster-based analysis also showed hemispherical laterlisation wherein the ipsilesional hemisphere possesses larger number of positively correlated clusters while contralesional hemisphere exhibits a contrasting characteristics. Moreover, this lateralization is more prominent within the anterior-posterior (i.e. Fronto-parietal) network involving superior frontal gyrus (SFG), inferior frontal gyrus (IFG), superior prietal gyrus (SPG), superior occipital gyrus (SOG), and medial occipital gyrus (MOG). The inter-hemispherical FC analysis showed a stable pattern of positively correlated connections within the motor cortical regions whereas the inter-hemispheric negative cluster is variable across the participant. For each participant, change in the values of FCs is estimated as follows:

$$MIM_{diff}^i = MIM_{post}^i - MIM_{pre}^i \qquad (7)$$

where MIM_{pre}^i and MIM_{post}^i are FC values for i^{th} ROI of pre- and post-intervention session. Furthermore, node strength
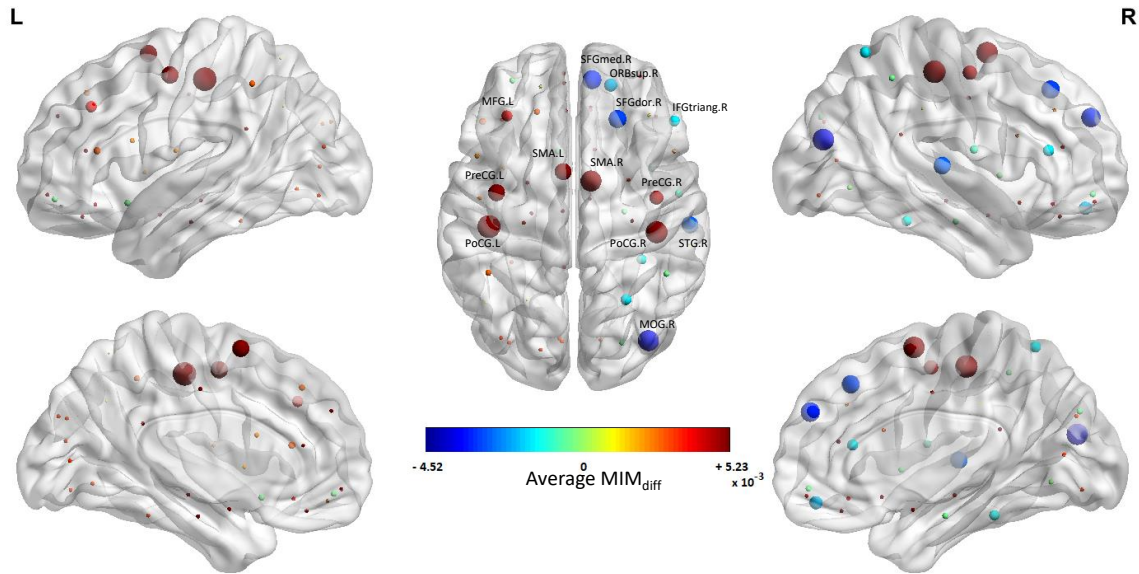
Fig. 7. The average node strengths (over the participants) for all significantly correlated (both positive and negative) ROIs estimated from the difference between the brain functional connectivity values of the pre-intervention and the post-intervention MEG scans. The nomenclature of the AAL atlas brain regions and their list of abbreviations are provided in Table S1 of the supplementary document. L: Left; R: Right; Ipsilesional hemisphere = Left

of all the significantly correlated ROIs were estimated by adding their associated FC values (one-to-all). Fig. 7 presents the average node strengths (across four participants) of all the significantly correlated ROIs. Thus, the group analysis showed increase in node strengths in the motor cortex region and decrease in the node strengths in the frontal, parietal and occipital areas of the contralesional hemisphere.

Table II provides the MNI coordinates and the average (over the four participants) node strengths of all the significantly correlated AAL Atlas based ROIs. The ROIs in the motor cortex area (i.e. precentral gyrus, postcentral gyrus and SMA) contribute largely to the increase in the information flow within the sub-network associated with the UL functional recovery. Likewise, frontal gyrus (SFGdor-L, MFG-L) and Inferior parietal lobule in the affected hemisphere also exhibit a similar pattern. On the contrary, brain regions in the frontal (SFGdor-R, ORBsup.R, IFGtriang-R, SFGmed-R), temporal (STG-R), and parieto-occipital (MOG-R, SPG-R) areas of the unaffected hemisphere provided major contribution to the reduction in FC strengths.

IV. DISCUSSION AND CONCLUSION

Assessment of functional recovery of upper extremities after stroke is highly crucial for restoring ADLs of the patients. Moreover, this assessment can not only validate the effectiveness of the rehabilitative intervention but may contribute to the development of better intervention designs. This study presented a functional connectivity-based neuro-physiological assessment of a multi-modal longitudinal (upto 6 weeks long) rehabilitative intervention involving the si-multaneous implementation of MA, BCI, visual as well as proprioceptive feedback, and robotic hand-exoskeleton. The whole-brain functional connectivity networks using RS MEG data and two different UL functional recovery measures (i.e.

ARAT and GS) were acquired for five different sessions over the complete intervention period. Furthermore, a cluster-based statistical analysis was implemented to discover the positively and negatively correlated sub-networks wherein Spearman rank correlation coefficients were estimated between the band-limited whole-brain RS MEG FC networks and the UL functional recovery index. This analysis yielded several major outcomes.

The behavioural assessment of the functional recovery showed gradual improvement in the ARAT and GS scores for all the four participants. A statistically significant increase in the overall ARAT score is obtained with the intervention, while improvements are well over the MCID for both mea-sures. Although, our previous work based on MI-BCI showed inconsistent improvement (over the participants) in both ARAT and GS measures [35], a more stable improvement in this current study may be explained by the major advancement of involving a combination of several rehabilitative modalities together.

The MEG connectivity analysis and the cluster-based sta-tistical testing have given several distinct patterns of brain functional connectome. The motor network involving precen-tral gyrus (i.e. M1), postcentral gyrus (i.e. S1), and SMA brain regions became stronger with UL functional recovery. Both M1 and S1 have been directly associated with motor learning and post-stroke functional recovery whereas SMA is known to play a crucial role in gait control and motor coordination [19], [61], [62]. A strengthened association of these three systems namely, the M1, S1, and the SMA in a functional network could be beneficial for motor recovery because it might constitute an adapted functional network for processing. Moreover, this pattern emerged in both ip-silesional and contralesional hemispheres of the brain, thus, depicting a bilateral hemispheric effect of the neuroreha-

bilitation intervention. The association of ipsilesional and/or contralesional hemispheres with UL functional recovery is still unclear with inconsistent findings reported elsewhere [34], [63], [64]. However, the bimanual implementation of MP and PP during the rehabilitative intervention may result in the bilateral hemispheric effect in this study. It is worth noting that this pattern exhibits inter-subject variability wherein even with significantly higher increase in GS values, participant P03 showed fewer positively correlated connections in the FCN cluster. This inter-subject variability may be a result of differences in terms of legion location and size, post-stroke lifestyle, initial upper-limb functional capacity (Baseline ARAT and GS values) and psychological factors such as motivation. Future studies involving larger sample size may consider exploring various factors related to inter-subject variability in relation to UL functional recovery among stroke patients. If possible, these studies can be aimed to establish a reliable criterion to distinguish responders from non-responders of FC based changes.

Interestingly, we have observed a lateralized reorganisation of a fronto-parietal network wherein the ipsilesional and the contralesional hemispheres showed enhanced and reduced connectivity strengths, respectively. Fronto-parietal connectivity is known to be involved in top-down attentional control and visuospatial processing [65]. Recently, its association with mobility has been established through a randomized controlled trial involving aerobic exercise [66]. However, the hemispheric lateralization showed specificity of the intervention effect on the FP network. As the intervention involves MA and robotics-guided physical movements, its effect may not only involve physical recovery but also cognitive functional recovery. However, further studies must be undertaken for in-depth assessment of the phenomena.

There are several limitations to be considered while considering the outcomes of this study. First, as the study involves the implementation of several rehabilitative modalities simultaneously, it is difficult to associate various outcomes with different modalities individually. Second, this study involved neurophysiological assessment of the intervention with stroke participants only and lacks the involvement of healthy individuals as a control group. Nevertheless, as the findings are based on the correlations estimated among the data of multiple sessions recorded over the intervention period, their scientific relevance is still sustained. Third, these findings must be verified with large sample size and larger intervention duration for further establishment of these neurophysiological patterns as biomarkers for the BMI-driven post-stroke UL functional recovery. Fourth, the trends within FCNs in association with subgroups of ARAT i.e. grip, grasp, pinch, and gross movement can be explored for further analysis. However, as the primary aim of this study is to capture the FCNs associated with overall upper limb functional recovery, we believe that considering the total ARAT score is more intuitive way of achieving this target. Moreover, to see the patterns for each subgroup, we have to treat the other subgroups as covariates which in turn require a bigger sample size. As one of the main constraints of our study is small sample size (discussed in previous point) i.e. five sessions only, analysing subgroup

level association of upper limb functional recovery with FCNs may not be feasible with this dataset.

REFERENCES

[1] E. S. Lawrence *et al.*, "Estimates of the prevalence of acute stroke impairments and disability in a multiethnic population," *Stroke*, vol. 32, no. 6, pp. 1279–1284, 2001.

[2] D. U. Jette *et al.*, "Physical therapy interventions for patients with stroke in inpatient rehabilitation facilities," *Physical therapy*, vol. 85, no. 3, pp. 238–248, 2005.

[3] D.-H. Bang *et al.*, "Effects of modified constraint-induced movement therapy with trunk restraint in early stroke patients: A single-blinded, randomized, controlled, pilot trial," *NeuroRehabilitation*, vol. 42, no. 1, pp. 29–35, 2018.

[4] S. A. Hays *et al.*, "Vagus nerve stimulation during rehabilitative training improves functional recovery after intracerebral hemorrhage," *Stroke*, pp. STROKEAHA–114, 2014.

[5] K. Takeda *et al.*, "Review of devices used in neuromuscular electrical stimulation for stroke rehabilitation," *Medical devices (Auckland, NZ)*, vol. 10, p. 207, 2017.

[6] Z. Yue *et al.*, "Hand rehabilitation robotics on poststroke motor recovery," *Behavioural neurology*, vol. 2017, 2017.

[7] G. Morone *et al.*, "Robot-assisted gait training for stroke patients: current state of the art and perspectives of robotics," *Neuropsychiatric disease and treatment*, vol. 13, p. 1303, 2017.

[8] M. A. Lebedev and M. A. Nicolelis, "Brain-machine interfaces: From basic science to neuroprostheses and neurorehabilitation," *Physiological reviews*, vol. 97, no. 2, pp. 767–837, 2017.

[9] S. R. Soekadar *et al.*, "Brain–machine interfaces in neurorehabilitation of stroke," *Neurobiology of disease*, vol. 83, pp. 172–179, 2015.

[10] A. Dionísio *et al.*, "The use of repetitive transcranial magnetic stimulation for stroke rehabilitation: A systematic review," *Journal of Stroke and Cerebrovascular Diseases*, vol. 27, no. 1, pp. 1–31, 2018.

[11] W. Klomjai *et al.*, "Repetitive transcranial magnetic stimulation and transcranial direct current stimulation in motor rehabilitation after stroke: an update," *Annals of physical and rehabilitation medicine*, vol. 58, no. 4, pp. 220–224, 2015.

[12] J.-Y. Park *et al.*, "The effect of mirror therapy on upper-extremity function and activities of daily living in stroke patients," *Journal of physical therapy science*, vol. 27, no. 6, pp. 1681–1683, 2015.

[13] S. Waghavkar and S. Ganvir, "Effectiveness of mirror therapy to improve hand functions in acute and subacute stroke patients," *Int J Neurorehabilitation*, vol. 2, no. 184, pp. 2376–0281, 2015.

[14] D. G. Carrasco and J. A. Cantalapiedra, "Effectiveness of motor imagery or mental practice in functional recovery after stroke: a systematic review," *Neurología (English Edition)*, vol. 31, no. 1, pp. 43–52, 2016.

[15] H. Liu *et al.*, "Mental practice combined with physical practice to enhance hand recovery in stroke patients," *Behavioural Neurology*, vol. 2014, 2014.

[16] L. Huang and G. van Luijtelaar, "Brain computer interface for epilepsy treatment," in *Brain-Computer Interface Systems-Recent Progress and Future Prospects*. InTech, 2013.

[17] G. Pfurtscheller *et al.*, "Changes in central EEG activity in relation to voluntary movement. ii. hemiplegic patients," in *Progress in brain research*. Elsevier, 1980, vol. 54, pp. 491–495.

[18] D. Rathee *et al.*, "Single-trial effective brain connectivity patterns enhance discriminability of mental imagery tasks," *Journal of neural engineering*, vol. 14, no. 5, p. 056005, 2017.

[19] B. Várkuti *et al.*, "Resting state changes in functional connectivity correlate with movement recovery for BCI and robot-assisted upper-extremity training after stroke," *Neurorehabilitation and Neural Repair*, vol. 27, no. 1, pp. 53–62, 2013.

[20] A. Paggiaro *et al.*, "Magnetoencephalography in stroke recovery and rehabilitation," *Frontiers in neurology*, vol. 7, p. 35, 2016.

[21] K. K. Ang *et al.*, "Brain-computer interface-based robotic end effector system for wrist and hand rehabilitation: results of a three-armed randomized controlled trial for chronic stroke," *Frontiers in neuroengineering*, vol. 7, p. 30, 2014.

[22] E. Buch *et al.*, "Think to move: a neuromagnetic brain-computer interface (BCI) system for chronic stroke," *Stroke*, vol. 39, no. 3, pp. 910–917, 2008.

[23] E. Biryukova *et al.*, "Recovery of the motor function of the arm with the aid of a hand exoskeleton controlled by a brain–computer interface in a patient with an extensive brain lesion," *Human Physiology*, vol. 42, no. 1, pp. 13–23, 2016.

[24] S. Kotov *et al.*, "Rehabilitation of stroke patients with a bioengineered "brain–computer interface with exoskeleton" system," *Neuroscience and Behavioral Physiology*, vol. 46, no. 5, pp. 518–522, 2016.

[25] O. Mokienko *et al.*, "Brain–computer interface: The first experience of clinical use in russia," *Human Physiology*, vol. 42, no. 1, pp. 24–31, 2016.

[26] A. Chowdhury *et al.*, "Online covariate shift detection based adaptive brain-computer interface to trigger hand exoskeleton feedback for neuro-rehabilitation," *IEEE Transactions on Cognitive and Developmental Systems*, 2017.

[27] K. K. Ang *et al.*, "A randomized controlled trial of EEG-based motor imagery brain-computer interface robotic rehabilitation for stroke," *Clinical EEG and neuroscience*, vol. 46, no. 4, pp. 310–320, 2015.

[28] A. Ramos-Murguialday *et al.*, "Brain–machine interface in chronic stroke rehabilitation: a controlled study," *Annals of neurology*, vol. 74, no. 1, pp. 100–108, 2013.

[29] T. Ono *et al.*, "Brain-computer interface with somatosensory feedback improves functional recovery from severe hemiplegia due to chronic stroke," *Frontiers in neuroengineering*, vol. 7, p. 19, 2014.

[30] F. Sergi *et al.*, "Predicting efficacy of robot-aided rehabilitation in chronic stroke patients using an MRI-compatible robotic device," in *Engineering in Medicine and Biology Society, EMBC, 2011 Annual International Conference of the IEEE*. IEEE, 2011, pp. 7470–7473.

[31] G. Andrew James *et al.*, "Changes in resting state effective connectivity in the motor network following rehabilitation of upper extremity poststroke paresis," *Topics in stroke rehabilitation*, vol. 16, no. 4, pp. 270–281, 2009.

[32] S. Bajaj *et al.*, "Brain effective connectivity during motor-imagery and execution following stroke and rehabilitation," *NeuroImage: Clinical*, vol. 8, pp. 572–582, 2015.

[33] B. M. Young *et al.*, "Changes in functional connectivity correlate with behavioral gains in stroke patients after therapy using a brain-computer interface device," *Frontiers in neuroengineering*, vol. 7, p. 25, 2014.

[34] G. Pellegrino *et al.*, "Inter-hemispheric coupling changes associate with motor improvements after robotic stroke rehabilitation," *Restorative neurology and neuroscience*, vol. 30, no. 6, pp. 497–510, 2012.

[35] G. Prasad *et al.*, "Applying a brain-computer interface to support motor imagery practice in people with stroke for upper limb recovery: a feasibility study," *Journal of neuroengineering and rehabilitation*, vol. 7, no. 1, p. 60, 2010.

[36] A. Chowdhury *et al.*, "An eeg-emg correlation-based brain-computer interface for hand orthosis supported neuro-rehabilitation," *Journal of neuroscience methods*, 2018.

[37] R. C. Lyle, "A performance test for assessment of upper limb function in physical rehabilitation treatment and research." *International Journal of Rehabilitation Research*, vol. 4, no. 4, pp. 483–492, 1981.

[38] S. Taulu and J. Simola, "Spatiotemporal signal space separation method for rejecting nearby interference in meg measurements," *Physics in Medicine & Biology*, vol. 51, no. 7, p. 1759, 2006.

[39] R. Oostenveld *et al.*, "Fieldtrip: open source software for advanced analysis of MEG, EEG, and invasive electrophysiological data," *Computational intelligence and neuroscience*, vol. 2011, p. 1, 2011.

[40] A. Hyvarinen, "Fast and robust fixed-point algorithms for independent component analysis," *IEEE transactions on Neural Networks*, vol. 10, no. 3, pp. 626–634, 1999.

[41] G. Barbati *et al.*, "Optimization of an independent component analysis approach for artifact identification and removal in magnetoencephalographic signals," *Clinical Neurophysiology*, vol. 115, no. 5, pp. 1220–1232, 2004.

[42] A. Delorme *et al.*, "Enhanced detection of artifacts in EEG data using higher-order statistics and independent component analysis," *Neuroimage*, vol. 34, no. 4, pp. 1443–1449, 2007.

[43] A. M. Dale *et al.*, "Cortical surface-based analysis: I. segmentation and surface reconstruction," *Neuroimage*, vol. 9, no. 2, pp. 179–194, 1999.

[44] B. Fischl *et al.*, "Cortical surface-based analysis: Ii: inflation, flattening, and a surface-based coordinate system," *Neuroimage*, vol. 9, no. 2, pp. 195–207, 1999.

[45] A. Gramfort *et al.*, "MNE software for processing MEG and EEG data," *Neuroimage*, vol. 86, pp. 446–460, 2014.

[46] M. S. Hämäläinen and R. J. Ilmoniemi, "Interpreting magnetic fields of the brain: minimum norm estimates," *Medical & biological engineering & computing*, vol. 32, no. 1, pp. 35–42, 1994.

[47] J.-Z. Wang *et al.*, "Magnetic source images determined by a lead-field analysis: the unique minimum-norm least-squares estimation," *IEEE Transactions on Biomedical Engineering*, vol. 39, no. 7, pp. 665–675, 1992.

[48] M. Fuchs *et al.*, "Linear and nonlinear current density reconstructions," *Journal of clinical Neurophysiology*, vol. 16, no. 3, pp. 267–295, 1999.

[49] A. Ewald *et al.*, "Estimating true brain connectivity from EEG/MEG data invariant to linear and static transformations in sensor space," *Neuroimage*, vol. 60, no. 1, pp. 476–488, 2012.

[50] L. Marzetti *et al.*, "Frequency specific interactions of MEG resting state activity within and across brain networks as revealed by the multivariate interaction measure," *Neuroimage*, vol. 79, pp. 172–183, 2013.

[51] A. K. Engel *et al.*, "Intrinsic coupling modes: multiscale interactions in ongoing brain activity," *Neuron*, vol. 80, no. 4, pp. 867–886, 2013.

[52] G. Nolte *et al.*, "Identifying true brain interaction from EEG data using the imaginary part of coherency," *Clinical neurophysiology*, vol. 115, no. 10, pp. 2292–2307, 2004.

[53] L. Marzetti *et al.*, "The use of standardized infinity reference in EEG coherency studies," *Neuroimage*, vol. 36, no. 1, pp. 48–63, 2007.

[54] J.-M. Schoffelen and J. Gross, "Source connectivity analysis with MEG and EEG," *Human brain mapping*, vol. 30, no. 6, pp. 1857–1865, 2009.

[55] K. Sekihara *et al.*, "Removal of spurious coherence in MEG source-space coherence analysis," *IEEE Transactions on Biomedical Engineering*, vol. 58, no. 11, pp. 3121–3129, 2011.

[56] N. Tzourio-Mazoyer *et al.*, "Automated anatomical labeling of activations in SPM using a macroscopic anatomical parcellation of the MNI MRI single-subject brain," *Neuroimage*, vol. 15, no. 1, pp. 273–289, 2002.

[57] E. S. Edgington, "Randomization tests," *The Journal of psychology*, vol. 57, no. 2, pp. 445–449, 1964.

[58] C. E. Han *et al.*, "Predicting age across human lifespan based on structural connectivity from diffusion tensor imaging," in *Biomedical Circuits and Systems Conference (BioCAS), 2014 IEEE*. IEEE, 2014, pp. 137–140.

[59] E. Glerean *et al.*, "Reorganization of functionally connected brain sub-networks in high-functioning autism," *Human brain mapping*, vol. 37, no. 3, pp. 1066–1079, 2016.

[60] C. E. Lang *et al.*, "Estimating minimal clinically important differences of upper-extremity measures early after stroke," *Archives of physical medicine and rehabilitation*, vol. 89, no. 9, pp. 1693–1700, 2008.

[61] M. Borich *et al.*, "Understanding the role of the primary somatosensory cortex: Opportunities for rehabilitation," *Neuropsychologia*, vol. 79, pp. 246–255, 2015.

[62] D. Rathee *et al.*, "Estimation of effective fronto-parietal connectivity during motor imagery using partial granger causality analysis," in *Neural Networks (IJCNN), 2016 International Joint Conference on*. IEEE, 2016, pp. 2055–2062.

[63] J. Wu *et al.*, "Connectivity measures are robust biomarkers of cortical function and plasticity after stroke," *Brain*, vol. 138, no. 8, pp. 2359–2369, 2015.

[64] I. Favre *et al.*, "Upper limb recovery after stroke is associated with ipsilesional primary motor cortical activity: a meta-analysis," *Stroke*, vol. 45, no. 4, pp. 1077–1083, 2014.

[65] M. Scolari *et al.*, "Functions of the human frontoparietal attention network: Evidence from neuroimaging," *Current opinion in behavioral sciences*, vol. 1, pp. 32–39, 2015.

[66] C. L. Hsu *et al.*, "The impact of aerobic exercise on fronto-parietal network connectivity and its relation to mobility: an exploratory analysis of a 6-month randomized controlled trial," *Frontiers in human neuroscience*, vol. 11, p. 344, 2017.